PM0.1 non-bouncing impactor (NBI) for ultrafine particle mass and number measurements

Wen-Cheng Gong, Nicolas Jidenko, Yang-Rei Li, Thi-Cuc Le, Jean-Pascal Borra, Chuen-Jinn Tsai

$PM_{0.1}$ non-bouncing impactor (NBI) for ultrafine particle mass and number measurements

Wen-Cheng Gong[1,2], Nicolas Jidenko[2*], Yang-Rei Li[1], Thi-Cuc Le[1], Jean-Pascal Borra[2], and Chuen-Jinn Tsai[1*]

[1]Institute of Environmental Engineering, National Yang Ming Chiao Tung University, Hsinchu, Taiwan

[2]Lab Phys Gaz & Plasmas, CNRS, Univ. Paris Sud, CentraleSupélec, Université. Paris-Saclay, F-91405, Orsay, France

[*]Corresponding Authors

[*]Tel: +886-3-5731880; Fax: +886-3-5727835; Email: cjtsai@nycu.edu.tw

[2*] Tel: +33-169153678; Email: nicolas.jidenko@universite-paris-saclay.fr

Abstract

This study designed and tested a 30 L/min $PM_{0.1}$ non-bouncing impactor ($PM_{0.1}$ NBI) for ultrafine particle (UFP) mass concentration measurement. The $PM_{0.1}$ NBI uses a wetted glass fiber filter with continuous water injection to maintain a clean surface, preventing particle loading and bounce effects. Lab tests showed the 30 L/min $PM_{0.1}$ NBI outperformed the $PM_{0.1}$ stage of NCTU micro-orifice cascade impactor (NMCI, non-rotating) with a silicon oil-coated aluminum foil substrate in collecting solid particles, as the particle collection efficiency of the latter decreased obviously with increasing particle aerodynamic diameter for particles larger than ca. 300 nm, an apparent particle bounce phenomenon. The ambient field tests showed very close UFP mass concentrations between the $PM_{0.1}$ NBI sampler (the $PM_{0.1}$

NBI preceded by 3 stages with 18, 10, and 2.5 micrometer cutoff sizes) and the reference rotating 10-stages NMCI with the difference of ±0.5 μg/m^3 only. In addition, the 3 L/min $PM_{0.1}$ NBI was combined with a condensation particle counter to measure the UFP number concentrations which were shown to be very close to those of the reference with the difference of ±5% only in the laboratory tests for loaded particle mass up to 300 μg. Good agreement was also found in the field tests. Therefore, the current 3 L/min $PM_{0.1}$ NBI and the future PM NBI with smaller flow rates (0.2-2.1 L/min) and larger cut-sizes (such as 0.4-0.9 μm) can be used as viable UFP classifiers for improving UFP measurement accuracy both in mass concentrations and number concentrations and reducing the maintenance needs for the UFP classifiers which are important to long-term sampling and monitoring.

Keywords: ultrafine particle, $PM_{0.1}$, cascade impactor, particle loading, particle bounce

1. Introduction

Exposure to air pollution is estimated to cause about seven million premature deaths every year and new air quality guidelines were updated in 2021 in which $PM_{2.5}$ daily and hourly AQG levels (air quality goal) were further lowered to 15 and 5 μg/m^3 from 25 and 10 μg/m^3, respectively, to help reduce $PM_{2.5}$ levels and decrease its health burden (WHO, 2021). Due to health concerns of UFPs (ultrafine particles or $PM_{0.1}$, particles with aerodynamic diameters, D_{pa}, smaller than 0.1 μm) (HEI, 2013; Ohlwein et al., 2019), BC/EC (black carbon or elemental carbon) (US EPA, 2019) and SDS (particles originating from sand and dust storms) (Querol et al., 2019), actions to enhance research on the UFP risks and develop the corresponding mitigation methods were summarized in qualitative good practice statements, despite insufficient data to provide recommendations for AQG levels and interim targets for these specific types of PM (WHO, 2021). Practices to integrate UFP monitoring into the existing air quality monitoring, prioritize UFP source emission control, and advance approaches to the assessment of exposure to UFP for epidemiological studies and UFP management are recommended (WHO, 2021).

Exposure assessment for UFPs is typically based on particle number concentrations (NCs) (Ohlwein et al., 2019), particle mass concentrations (MCs) (Kumar et al., 2021), or lung-deposited surface area (Geiss et al., 2016). Among them, NC is the most common choice because the related measurement technologies are well-established (WHO, 2021), and UFPs are the main contributors to the total number of particles in the atmosphere (Morawska et al., 2008; Chen et al., 2010a). For the size distribution measurement of submicron particles including UFPs, a scanning mobility particle sizer (SMPS) incorporating a single-stage inlet impactor, an electrostatic classifier and a condensation particle counter (CPC), is the most commonly used instrument. The impactor removes particles larger than a known D_{pa} which sets the upper limit of the SMPS, thereby easing the multiple charge correction in the data inversion program (He and Dhaniyala, 2013). However, the high cost and complexity of the

SMPS limit its widespread use in large-scale UFP monitoring networks (Abdillah and Wang, 2023). In addition, the inlet impactor without a coated impaction substrate or with a silicone oil-coated substrate is known to be affected by particle bounce and loading effects (Le and Tsai, 2017; 2021). Therefore, regular maintenance is needed to keep its size-classifying performance accuracy during long-term monitoring and when particle concentration is high, such as in a highway tunnel (Chen et al., 2010a and 2010b) or welding booth (Chang et al., 2013), where $PM_{2.5}$ and UFP MCs can be as high as 78 and 33.2 μg/m^3, or 1,500 and 430 μg/m^3, respectively.

For physicochemical and toxicity assessment of UFPs (Chen et al., 2010b; Tsai et al., 2011; Kumar et al., 2021), mass-based measurement is required with a minimum sample mass of 100 μg and 1000 μg for the former and latter, respectively (Kumar et al., 2021). This amount of UFP sampling can be achieved in the high-concentration tunnels and workplace environments mentioned above, but it is a challenge in ambient settings where UFP concentrations are typically low, e.g. 2.2 μg/m^3 in roadside (Chen et al., 2010b), 0.7 μg/m^3 in forest (Chen et al., 2010b), and <0.5 μg/m^3 in California city (Xue and Kleeman, 2022), unless extended periods up to a few days or at high flow rates are used (Kumar et al., 2021; Xue et al., 2020). Most UFP samplers with high flow rates are cascade impactors that operate at flow rates ranging from several hundreds to 1100 liters per minute, and the $PM_{0.1}$ stage in these samplers is usually preceded by two to three stages, such as the high-volume ultrafine particle sampler (550 L/min, 2 stages: 2.5 and 0.15 μm) (Misra et al., 2002), the harvard high-volume cascade impactor (850 L/min, 3 stages: 2.4, 0.9 and 0.2 μm) (Sillanpaa et al., 2003), and the high-volume impactor Sampler (400 L/min, 2 stages: 2.5 and 0.18 μm) (Saleh et al., 2019). However, the D_{pa50} of the $PM_{0.1}$ stage in these samplers is 0.15, 0.2, and 0.18 μm only, respectively, which are considered quasi-UFPs but not true UFPs (Xue and Kleeman, 2022; Kumar et al., 2021; Sotty et al., 2019). Quartz fiber substrate used in the $PM_{0.1}$ stage of high-volume ultrafine particle sampler eliminates initial particle bounce, but the maximum

loaded particle mass (M_L) is limited to 60 mg, while the polyurethane foam substrate in harvard high-volume cascade impactor can increase the M_L but the particle collection efficiency curve is less steep than that of the flat substrate, as the air can penetrate into the porous substrate leading to increased collection of large particles due to inertia impaction and UFPs due to diffusion. (Huang et al., 2001; Sillanpaa et al., 2003; Huang and Tsai, 2005). Therefore, a silicon oil-coated smooth impaction surface is a better choice to achieve a more accurate measurement, especially for the classification of nanoparticles (Chen et al., 2018), but particle bounce and loading effects still need to be overcome (Le and Tsai, 2017; Le et al., 2022).

The UFPs measurement can be achieved using samplers that operate at a medium flow rate of 9 to 40 L/min (Chen et al., 2010a and 2010b; Kumar et al., 2021), such as the micro-orifice uniform deposit impactor (MOUDI, 30 L/min, Marple et a., 1991), the NCTU micro-orifice cascade impactor (NMCI, 30 L/min, Liu et al., 2013; Chien et al., 2015), and the nanosampler (40L/min, Furuuchi et al., 2010;). The $PM_{0.1}$ stage in the former two devices is preceded by a 0.18 μm-stage while nanosampler is preceded by a 0.5 μm-stage. MOUDI and NMCI employ rotating stages and silicon oil-coated substrates to increase the M_L, but the rotating feature does not exist in both high-volume UFP samplers and nanosampler. The mass collected on each stage of the MOUDI is limited to 3 mg (Marple et al., 1991) because the coating layer becomes ineffective with particle accumulation and particle bounce may occur from particle mounds (Tsai and Cheng, 1995; Misra et al., 2002).

For personal sampling of UFPs in workplaces, our group has developed a personal nanoparticle sampler (PENS, Tsai et al., 2012) which consists of a $PM_{4.0}$ cyclone-inlet and a micro-orifice impactor with D_{pa50} of 100 nm. Nevertheless, there is a M_L limit of 1.78 mg. To eliminate the particle loading effect, a 3.0 L/min NIC (Nanoparticle Inertial Classifier, Le et al., 2022) which is based on the non-bouncing feature of 16.7 L/min $PM_{2.5}$ M-WINS (modified well impactor ninety-six, Le and Tsai, 2017; Le et al., 2020), was developed in

which clean water is injected continuously at 0.3 mL/min flow rate (or vacuum oil is applied once per day for one minute at 3 mL/min each time) upward through a small drilled hole (1 mm diameter) located at the center of the glass fiber filter (GFF) impaction surface to wash off the deposited particles. The spent water/oil is then drained off from the hole at the edge of the impaction surface. The impaction substrate is thus free from loaded particle accumulation.

In this study, the non-bouncing impactor technique of our group was employed to modify the 9th stage of the NMCI (Liu et al., 2013) as the 30 L/min $PM_{0.1}$ Non-Bouncing Impactor (30 L/min $PM_{0.1}$ NBI) for UFP MC measurement, in particular for long-term sampling if enough UFP mass is desired. The NIC developed previously (hereafter called as 3 L/min $PM_{0.1}$ NBI) was used to replace the traditional impactor at the inlet of CPC or SMPS for long-term UFP NC measurement. The performance of these $PM_{0.1}$ NBIs was tested for the particle loading effect both in the laboratory and in an ambient environment using the 10-stage NMCI and SMPS as the references for MC and NC measurements, respectively.

2 Experimental methods

2.1 UFP MC measurement

Design of 30 L/min $PM_{0.1}$ NBI and sampling system

The 30 L/min $PM_{0.1}$ NBI is designed by modifying the 9th stage ($PM_{0.1}$ stage) of the NMCI, which consists of a nozzle plate having 2000 nozzles with a nozzle diameter of 55 μm and an impaction plate covered by a 37-mm GFF (Model TE-G653-37, TISCH) as shown in Fig. 1a. De-ionized water is injected by a peristaltic pump continuously upward via a 1-mm hole (internal diameter) drilled through the impactor plate and GFF with a flow rate of 0.5 mL/min to wet the GFF and remove deposited particles. Spent water then flows into the annular cavity around the impaction plate and is drained by another peristaltic pump. The 30 L/min $PM_{0.1}$ NBI was used for the particle collection efficiency test in the laboratory test while a complete 30 L/min $PM_{0.1}$ NBI sampler (NBIS) shown in Fig. 1b was used for the

particle loading and field tests. The 30 L/min $PM_{0.1}$ NBIS consists of the 30 L/min $PM_{0.1}$ NBI, preceded by 3 non-rotating impaction stages: the inlet stage (D_{pa50} of 18 μm), the first stage (D_{pa50} of 10 μm), and the second stage (D_{pa50} of 2.5 μm) followed by an after filter (47-mm Teflon filter, Model R2PL047, Pall) to collect UFP. The three preceding stages are used to remove coarse particles to avoid nozzle clogging in the $PM_{0.1}$ stage. The first two stages are the same as those of the NMCI while the diameter of 10 nozzles of the 2nd stage was reduced to 2.1 mm and re-calibrated to be 2.5 μm as will be shown in a later publication.

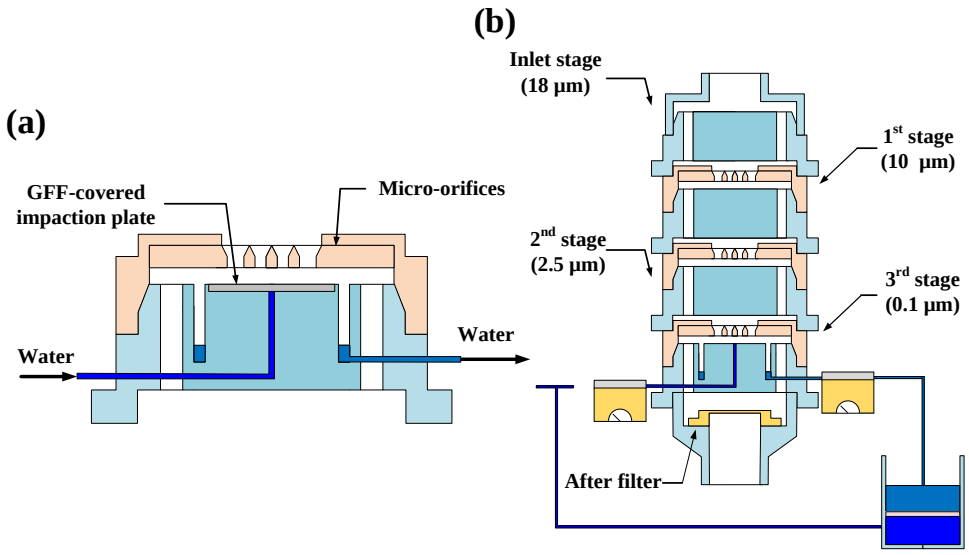

Fig. 1. Schematic diagram of the (a) 30 L/min $PM_{0.1}$ NBI (b) 30 L/min $PM_{0.1}$ NBI sampler (NBIS), non-rotating

Particle collection efficiency test

The experimental setup used for testing the particle collection efficiency of the 30 L/min $PM_{0.1}$ NBI is depicted in Fig. S1 (Section B) of the supplementary information (SI) and is similar to the one described in Le et al. (2022). Liquid dioctyl sebacate (DOS) and solid NaCl particles were generated by the evaporation-condensation method and by an atomizer followed by a diffusion dryer, respectively. The generated particles were charge neutralized and classified into monodisperse particles by a differential mobility analyzer (Model 3081, TSI). The particle concentrations were measured upstream and downstream of the NBI by

using a home-made faraday-cup with an electrometer (Model 6514, Keithley) to determine the particle collection efficiency (η, %) calculated by (Le et al., 2022):

$$\eta = (1 - \frac{I_{down}}{I_{up}}) \times 100 \quad (1)$$

where I_{up} and I_{down} is the upstream and downstream particle currents (μA), respectively. Then, the particle collection efficiency curve and D_{pa50} were determined by fitting the measured data using the following equation (Le et al., 2022; Le and Tsai, 2017):

$$\eta(D_{pa}) = 100\% - a - b\left[1 - \left[1 + \exp\left(\frac{D_{pa} + d\ln\left(2^{\frac{1}{e}} - 1\right) - c}{d}\right)\right]^{-e}\right] \quad (2)$$

where a, b, c, d, and e are the fitting parameters. The classification curve sharpness (κ) was also calculated as the square root of the ratio of D_{pa84} and D_{pa16} which correspond to the particle collection efficiency of 84% and 16%, respectively. In addition, a single 9th stage of the NMCI was also tested for comparison, where the impaction substrate is the silicone oil (Model KF96SP, Shin-Etsu Chem. Co., Ltd., Japan)-coated aluminum foil substrate (47mm, Allfield Ltd., Taiwan).

Particle loading test in the laboratory

The experimental setup of the particle loading test of the 30 L/min $PM_{0.1}$ NBIS is depicted in Fig. S2 (Section B) of the SI. For comparison, a 30 L/min traditional cascade impactor-R (TCI-R)) consisting of rotating stages 0, 1, 2 and 9 (the cut-sizes of 18, 10, 2.5 and 0.1 μm, respectively) of the NMCI and an after filter (47-mm Teflon filter, Model R2PL047, Pall) was also tested. All 4 stages of the TCI-R use rotating and silicon oil-coated

aluminum foil substrates. Similar to the 30 L/min $PM_{0.1}$ NBIS, the $PM_{0.1}$ stage of the TCI-R was preceded by the $PM_{2.5}$ stage to examine the possible particle loading effect which may also occur in High-Volume UFP samplers described earlier. The quasi-UFP stages of these samplers are all preceded by an upper stage with 0.9 to 2.5 μm as the cutoff size.

The particle loading tests were conducted using nano-TiO_2 particles (AERODISP P25, Degussa, Germany) which were dried in an oven at 105°C for 2 hours before use. Particles were dispersed using a small-scale powder disperser (SSPD, Model 3433, TSI) and then introduced to the NBIS and TCI-R for $PM_{0.1}$ MC measurement by weighing the particle masses on the after filters before and after each test. Based on experimental data of the SSPD-dispersed nano-TiO_2 particles, which showed UFP and TSP mass concentrations to be 92 and 3,427 $\mu g/cm^3$, respectively (Le et al., 2022), the UFP/TSP fraction is calculated to be 2.68%. As these particles were reported to have stable mass and number size distributions (Tsai et al., 2012; Le et al., 2022), the UFP/TSP fraction of 2.68% is assumed to remain constant in this study and is used for comparison with measurements from the NBIS and TCI-R in this loading test.

The M_L of the $PM_{0.1}$ stage of the TCI-R was obtained by weighing the silicone oil-coated aluminum foil substrates before and after the tests. The M_L of the NBIS-$PM_{0.1}$ stage was calculated using the formula ((TSP × $PM_{2.5}$/TSP ratio) - $PM_{0.1}$) (unit: mg). Note that the TSP value was obtained from a 5 L/min filter cassette containing a 47-mm Teflon filter, which was collocated with the NBIS and TCI-R. The particle loading effect of the NBIS and TCI-R was checked by the relationship of the measured UFP MCs with different M_L and compared with the reference UFP values.

Field test in ambient conditions

The field comparison tests were performed on the roof of the Institute of Environmental Engineering at National Yang Ming Chiao Tung University. The roof is situated 20 meters

above the ground and is close to the Hsinchu Science Industrial Park and the main roads of Hsinchu City, where there is heavy traffic flow during the morning and evening rush hours. The 30 L/min $PM_{0.1}$ NBIS, 10-stage rotating NMCI, and TCI-R were used in the test as shown in Fig. S3 (Section B) of the SI. In addition, the TCI-NR (i.e., the TCI with non-rotating silicon oil-coated aluminum foil substrate) instead of TCI-R was also tested for comparison purposes. Two comparison tests were conducted, test-1 was to compare the NBIS, NMCI, and TCI-R, while test-2 was to compare the NBIS, NMCI, and TCI-NR. Four and five 24-hr average UFP samples were collected for test-1 and test-2, respectively from December 2021 to March 2022, when daily average $PM_{2.5}$ concentration varied from 10 to 40 $\mu g/m^3$, temperature varied from 14 to 24 °C, and relative humidity varied from 62 to 75%.

The M_L on the $PM_{0.1}$ stage of the TCI-R or -NR was obtained by weight gain on the stage, while the M_L on the $PM_{0.1}$ stage of the NBIS was calculated using the formula ($PM_{2.5}$ mass in the NMCI - $PM_{0.1}$ mass in NBIS). It is worth noting that the relative percent differences (RPD) of the $PM_{2.5}$ MCs measured by the NMCI, TCI-R, and -NR average 6.2% as shown in Table S1 (Section A), implying the accuracy of the comparison tests. The accuracy of the $PM_{0.1}$ measurement was evaluated based on comparing the $PM_{0.1}$ MCs measured by the tested devices with those of the NMCI as the reference.

2.2 UFP NC measurement

The UFP NC or size distribution monitoring system, shown in Fig. S4 (Section B) of the SI, uses the 3 L/min $PM_{0.1}$ NBI as the inlet of a commercial CPC (Model 3788, TSI) or a SMPS (Model 3936, TSI), respectively. The systems for UFP NCs or size distribution measurement are named NBI-CPC or NBI-SMPS. Because the flow rate of the $PM_{0.1}$ NBI is 3 L/min, 2.4/2.7 L/min has to be bypassed when the inlet flow rate of CPC/SMPS is 0.6/0.3 L/min.

Particle loading test in the laboratory

The effect of loaded particle mass (M_L) of the 3 L/min NBI is examined by the relationship of the ratio of the UFP NCs of the NBI-CPC to those of the reference SMPS with various M_L. Here the SMPS is used as the reference instrument where a TSI inlet impactor (nozzle diameter: 0.0457 cm) was first tested for the particle loading effect to determine the acceptable M_L of 150 μg before use. The inlet impactor was cleaned before the M_L exceeded the acceptable value to maintain good classification performance.

The experimental setup of the particle loading test for the SMPS's TSI inlet impactor is shown in Fig S5 (Section B) of the SI. The SMPS equipped with a 0.0457 cm-nozzle inlet impactor (D_{pa50}: 410 nm) was operated at an aerosol flow of 0.6 L/min and a sheath flow of 3 L/min. The polydisperse NaCl particles were introduced into the SMPS to measure the particle number distribution, which was recorded over time. The particle loading effect of the SMPS inlet impactor was evaluated based on the variation of the particle number distribution with loaded particle mass (M_L) which was obtained by determining the mass difference of the impaction substrate by weighing before and after each loading test.

The experimental setup of the particle loading test of the NBI coupled with the CPC is shown in Fig. S6 (Section B) of the SI. Similar to the particle loading test of the SMPS inlet impactor, the generated NaCl particles were introduced simultaneously into the collocated NBI-CPC and SMPS to measure the UFP NC and number size distribution, respectively. The SMPS used in this test applies a 0.3 L/min CPC (Model 3776, TSI), in which the SMPS inlet impactor (nozzle size of 0.0457 cm) has a D_{pa50} of 615 nm. As the D_{pa50} is much larger than 100 nm, the UFP measurement in SMPS is not affected (He and Dhaniyala, 2013). The effective density used for the conversion of the electrical mobility diameter (D_{pe})-based SMPS data to the D_{pa}-based values using the conversion equation Eq. S1 in Section C of the SI, is 1.7 g/cm^3 for NaCl particles. The M_L was determined by integrating the mass distribution converted from the number distribution with the details provided in Section D of

the SI. A traditional impactor (TI, i.e., the 3 L/min $PM_{0.1}$ NBI used a silicone oil-coated aluminum substrate instead of the water-wetted GFF) used as the inlet of the CPC was also tested for comparison.

Field comparison test

The field comparison test of the 3.0 L/min NBI-CPC versus the SMPS as the reference was carried out at the same location as that of 30 L/min $PM_{0.1}$ NBIS test, and lasted for five days (08-13 Jan 2023). Fig. S7 (Section B) of the SI shows the test setup which consists of a PM_{10} inlet and a Very Sharp Cut Cyclone $PM_{2.5}$ inlet (Le et al., 2020) followed by NBI-CPC and SMPS. After $PM_{2.5}$ inlet, the 16.7 L/min air flow was split into three streams: 3 L/min for the NBI-CPC, 0.3 L/min for the SMPS, and 13.4 L/min for the bypass flow. The UFP NCs were measured by the NBI-CPC and compared with the reference values (i.e. NCs of D_{pa} smaller than 100 nm) determined from the particle number distribution (D_{pe} of 14-700 nm) monitored by the SMPS. The effective density used for the size conversion is chosen to be 1.2 g/cm^3, which is typical in an urban environment (Liao et al., 2019).

3. Results and Discussion

3.1 UFP MC measurement

Particle collection efficiency test in the laboratory

Fig. 2 shows the particle collection efficiency curves of the 30 L/min $PM_{0.1}$ NBI and 9th stage of the NMCI for different particle types. The $PM_{0.1}$ NBI has D_{pa50} of 107 nm and κ of 1.60 for solid NaCl particles, and D_{pa50} of 108 nm and κ of 1.62 for liquid DOS particles, demonstrating good cut-off performance with the cut-size close to the expected 100 nm (Le et al., 2022). In comparison, the NMCI-$PM_{0.1}$ stage (9th stage) also shows good classification performance for liquid DOS particles with a cut-size of 108 nm and κ of 1.71, which agrees well with the test results for liquid particles in the previous studies (Liu et al., 2013; Chien et

al., 2015). For solid NaCl particles, D_{pa50} and κ of the NMCI-$PM_{0.1}$ stage are also 107 nm and 1.87, respectively, similar to those of the 30 L/min $PM_{0.1}$ NBI sampler, but the particle collection efficiencies become lower than those of liquid particles when particles are larger than the cut-size. The decrease in the collection efficiency becomes much more obvious as D_{pa} is larger than 300 nm due to solid particle bounce in the NMCI-$PM_{0.1}$ stage with the rotating, silicone oil-coated aluminum foil substrate. In the NMCI-$PM_{0.1}$ stage with silicone-oil coated

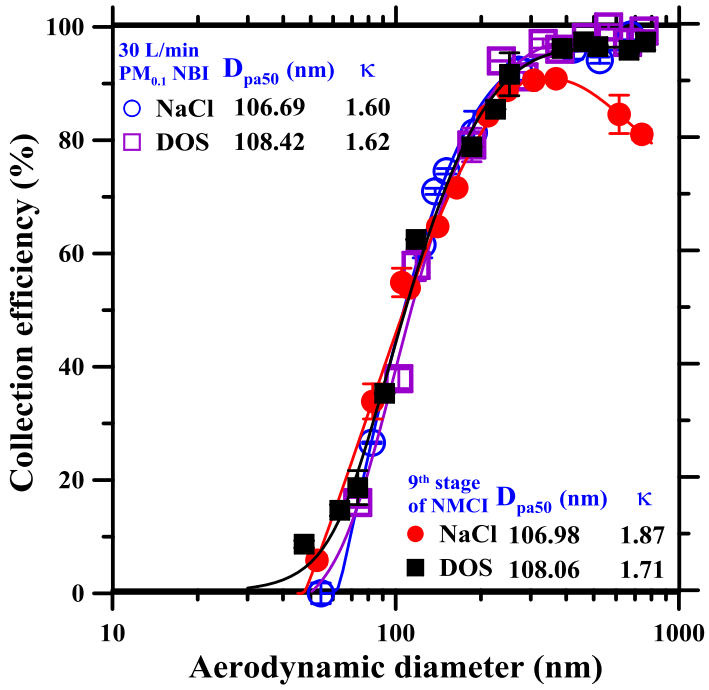

Fig. 2. Particle collection efficiency of the $PM_{0.1}$ stage of the NBIS and 9th stage of the NMCI

aluminum substrate, an oil-free spot is formed under each nozzle since the air jet velocity is as high as 144 m/s resulting in particle bounce similar to that observed in the previous study of our group (Tsai et al., 2012) in which a silicone-oil coated Teflon filter (10 μm pore size) had to be used to resolve this issue and prevent particle bounce. The Teflon filter has a uniform micro-pore structure, which facilitates capturing and retaining liquid within its pores throughout surface (Turner and Hering, 1987). Similar phenomena have been observed in

other substrate materials having micro-porous structure, such as oil-soaked sintered metal disks (Reischl and John, 1978). Besides, continuous water injection at the center of the substrate helps maintain a steady supply of water to keep the GFF surface wet (Le et al., 2022). Therefore, the air jet won't push water aside and leave a dry spot beneath each of the nozzles.

However, solid particle bounce does not occur easily in the 10-stage NMCI, in which the $PM_{0.1}$ stage is preceded by the 0.18-μm stage (8^{th} stage). Only particles smaller than 180 nm are collected on the $PM_{0.1}$ stage thereby eliminating possible particle bounce effect. But if a traditional $PM_{0.1}$ impactor is preceded by a upstream stage with a cut-size larger than about 0.2~0.3 μm, such as 0.5 μm in nanosampler (KANOMAX, Japan) (Furuuchi et al., 2010) or 0.9-2.5 μm in the high-volume UFP impactors, it is very likely that particle bounce could occur on the $PM_{0.1}$ stage leading to overestimation of UFP MCs. This will be demonstrated in the following section where the test results of 4-stage TCIs, whose $PM_{0.1}$ stage is preceded by the $PM_{2.5}$ stage, are shown.

Particle loading test in the laboratory

Fig. 3 shows the $PM_{0.1}$ MCs measured by the NBIS and TCI-R at various nano-TiO_2 M_L. Since the source generating particles was stable during the test, the inlet $PM_{0.1}$ concentration can be assumed to be constant and is calculated to be 105.46 μg/m^3 (based on the measured TSP concentration of 3.93 mg/m^3 × $PM_{0.1}$/TSP ratio of 2.68%). This inlet concentration value is used as the reference, represented as the solid line in Fig. 3, to evaluate the performance of the NBIS and TCI-R.

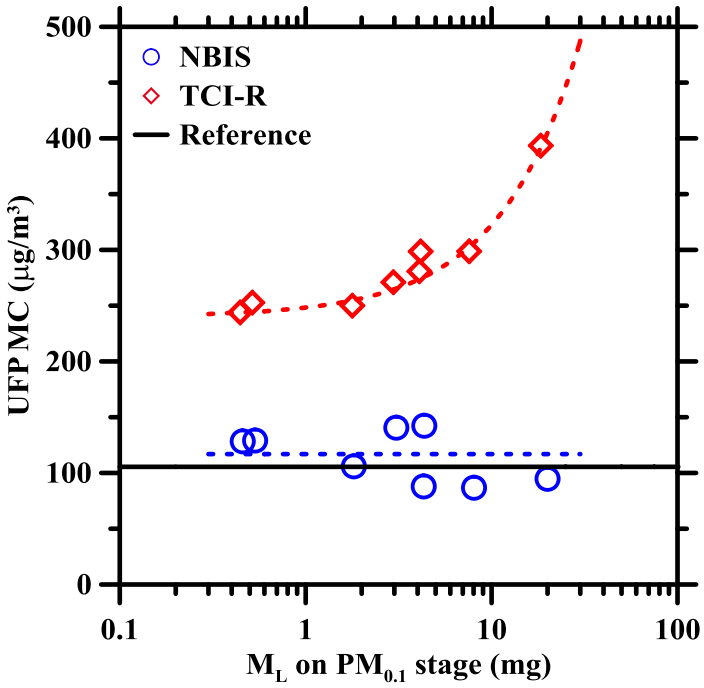

Fig. 3. UFP MC by the NBIS and TCI-R versus M_L.

Initially, the TCI-R measures $PM_{0.1}$ MC of 244 μg/m^3 at an M_L as low as 0.44 mg, which is much higher than the reference value of 105.46 μg/m^3. It indicates an over-measurement problem of the TCI-R with the rotating, silicon oil-coated impaction substrate. The initial over-measurement occurs due to the "initial bounce" for particles larger than 300 nm from the $PM_{0.1}$ stage, which is explained earlier in the previous section. Subsequently, the measured $PM_{0.1}$ MC of the TCI-R increases slightly to 268 μg/m^3 from 244 μg/m^3 when the particle mass load is increased to 2.96 mg from 0.44 mg.

The acceptable M_L limit of 3.0 mg was suggested by Marple et al. (1991). When the M_L is increased from 3.0 to 18.38 mg, the measured $PM_{0.1}$ MC is increased to 394 μg/m^3, or 1.6 times the initial value. This indicates particle overloading effect induces more particle bounce in the TCI-R when the M_L exceeds 3 mg. Therefore, the use of a preceding stage with D_{pa} < 300 nm is needed for the $PM_{0.1}$ TCI-R to prevent initial solid particle bounce and its impaction substrate needs to be cleaned and re-oiled regularly to prevent the over-measurement.

In comparison, NBIS measures the $PM_{0.1}$ concentration of 128 μg/m^3 at an M_L of 0.46 mg, which is close to the reference value of 105.46 μg/m^3. The small difference in MCs is attributed to the experimental uncertainty of the low collected mass (<20 μg). It indicates that the NBIS has no initial particle bounce since the water-wetted GFF impaction substrate retains water effectively in the pores to prevent solid particle bounce. When the M_L is increased to 20.01 mg, the NBIS $PM_{0.1}$ MC still keeps at 94.74 μg/m^3. The average MC is 117±22 μg/m^3 for M_L ranging from 0.46 to 20.01 mg, which is within 10% bias compared to reference value. Therefore, the 30 L/min $PM_{0.1}$ NBIS has no particle bounce and loading effects, and is capable of sampling $PM_{0.1}$ MC at high concentration environments with good accuracy.

Field comparison test

The performance of the NBIS and TCIs (rotating or non-rotating stages) in the ambient air with low particle MCs is also tested. Fig. 4 displays the ambient $PM_{0.1}$ MCs measured by three devices, NBIS, TCI-R, and TCI-NR, versus reference $PM_{0.1}$ MCs measured by the rotating 10-stage NMCI. The results show that the NBIS $PM_{0.1}$ MCs vary from 0.68 to 2.41 μg/m^3, which are close to the NMCI $PM_{0.1}$ MCs ranging from 0.44 to 2.79 μg/m^3 with the concentration difference of less than ±0.5 μg/m^3 (difference averages only -0.02±0.36 μg/m^3). The linear regression analysis shows a high accuracy (slope=0.97) and a medium correlation (R^2=0.68) of the NBIS with the NMCI. This means that the NBIS can measure $PM_{0.1}$ MC accurately even in low UFP concentration environments.

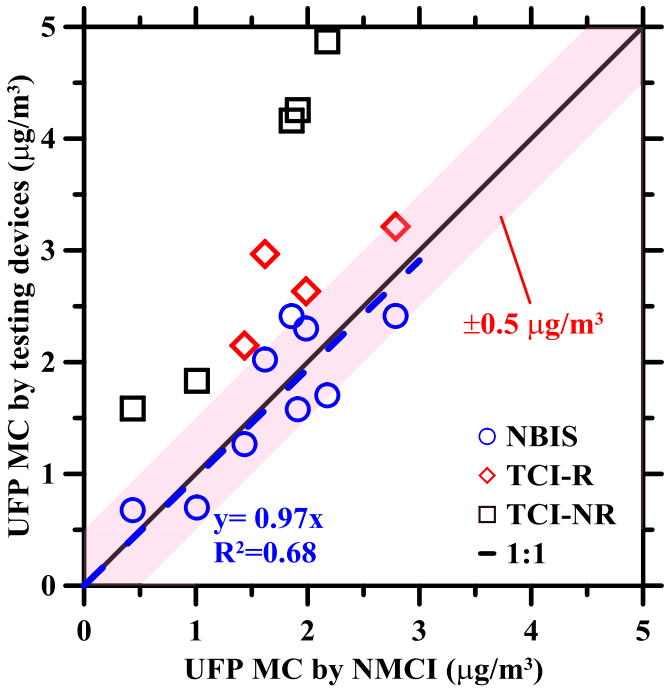

Fig. 4. Comparison of the UFP MC by the TCI and NBIS to the NMCI

In comparison, the TCI-R measures the $PM_{0.1}$ MCs of 2.15 to 3.21 μg/m^3 when the corresponding NMCI $PM_{0.1}$ MCs range from 1.44 to 2.79 μg/m^3. It is seen that the concentration difference between the TCI-R and NMCI exceeds ±0.5 μg/m^3 and the TCI-R $PM_{0.1}$ MCs are persistently higher than the NMCI $PM_{0.1}$ levels. It indicates the over-measurement of the TCI-R occurs due to the bounce for particles larger than 300 nm since its $PM_{0.1}$ stage is preceded by the stage with 2.5 μm cut-size, which is much larger than 300 nm. The average concentration difference is slightly higher at 0.78±0.34 μg/m^3 for all sampling days since no severe particle bounce caused by particle overloading effect as the M_L on $PM_{0.1}$ stage, <1.2 mg, is low.

In contrast, the TCI-NR measures the $PM_{0.1}$ MCs of 1.59 to 4.87 μg/m^3 when the NMCI $PM_{0.1}$ MCs values vary from 0.44 to 2.18 μg/m^3. As shown clearly in Fig. 4, the over-measurement of the TCI-NR is serious with the concentration difference of 0.82 to 2.69 μg/m^3 when the M_L on the $PM_{0.1}$ stage is less than 1.2 mg. This is because the particle bounce in the traditional $PM_{0.1}$ impactor with the non-rotating substrate is more severe than that with

the rotating substrate, which was found in our previous study (Tsai et al., 2012). In addition, over-measurement becomes more serious with the increase in ambient $PM_{0.1}$ concentration due to particle mounds formed underneath the nozzles resulting in a serious particle overloading effect.

The difference in the UFP MC measurement performance between TCI-R and TCI-NR can be explained by the difference in the particle deposited areas on the substrates, which can be calculated as the sum of projection areas of all nozzles (diameter of nozzle=55 μm, number of the nozzle=2000) in the TCI-NR and the nozzle distribution area of 25 mm in the TCI-R (Feng et al., 2016). Without rotating the substrate, the TCI-NR has a particle deposited area of $4.60*10^{-6}$ m^2 while the TCI-R with the rotating substrate has an area of $4.91*10^{-4}$ m^2, which is approximately 100 times that of the former. Therefore, M_L per unit deposition area on the $PM_{0.1}$ stage of TCI-R is much smaller than the one of TCI-NR. However, this rotating feature does not exist in all high-volume UFP samplers and Kanomax nanosampler, in addition to the afore-mentioned problems associated with the cut-size much larger than 300 nm for the $PM_{0.1}$ preceding stage.

3.2 UFP NC measurement

Particle loading test in the laboratory

Fig. 5 shows the particle number distribution measured by the SMPS with a 0.0457 cm-nozzle inlet impactor at various M_L. Initially, the particle number distribution has the CMAD, GSD, and total NCs of 56 nm, 1.8, and 8.0E06 #/cm^3, respectively. However, with the increase in M_L to 150 and 680 μg, the total NCs are decreased to 7.3×10^6 and 7.0×10^6 #/cm^3, respectively, which is 9 and 14% lower than the initial value. The decrease in particle NC is due to the particle loading effect owing to the particle mound formed on the impaction substrate (Le and Tsai, 2017; 2021). Particles smaller than the cut-size are collected as the jet-to-plate distance was shortened. As shown in Fig. 5, the particle mound at the M_L of 680

μg is larger and higher than the one at the M_L of 150 μg, indicating particle loading effect becomes worse leading to lower NCs. The present test results for the TSI inlet impactor (data not shown) also confirm that the D_{pa50} is decreased from the initial value of 410 nm (flow rate:0.6 L/min) to 360 and 348 nm as the M_L is increased from 0 to 150 and 480 μg, respectively, leading to the NC under-measurement by the SMPS. Therefore, the SMPS inlet impactor with a nozzle size of 0.0457 cm needs to be cleaned regularly when the M_L exceeds 150 μg to maintain a good performance with an acceptable bias of 10%.

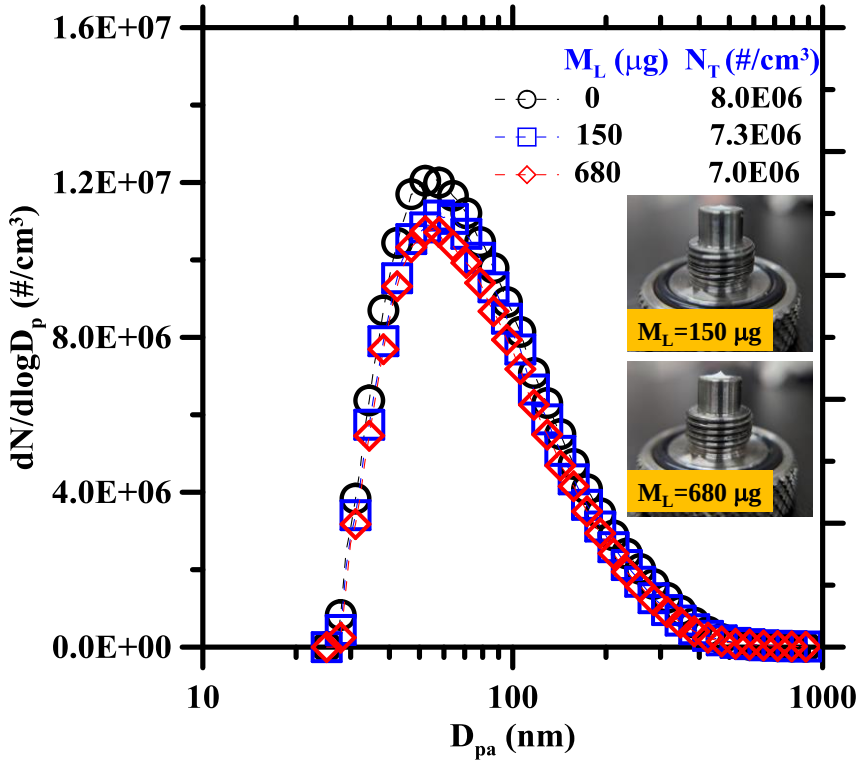

Fig. 5 The particle distribution by the SMPS with the TSI inlet impactor (nozzle: 0.0457 cm) at various loaded masses.

After determining the acceptable M_L of 150 μg of the SMPS impactor, the comparison tests of the NBI-CPC, TI-CPC and SMPS were conducted, during which the SMPS impactor was cleaned every 5 min to eliminate the particle loading effect. Fig. 6 presents the ratios of the $PM_{0.1}$ NCs measured by the NBI-CPC and TI-CPC to those of the SMPS at different M_L

of NaCl particles. The ratio of the $PM_{0.1}$ NCs measured by the TI-CPC to the SMPS is found to

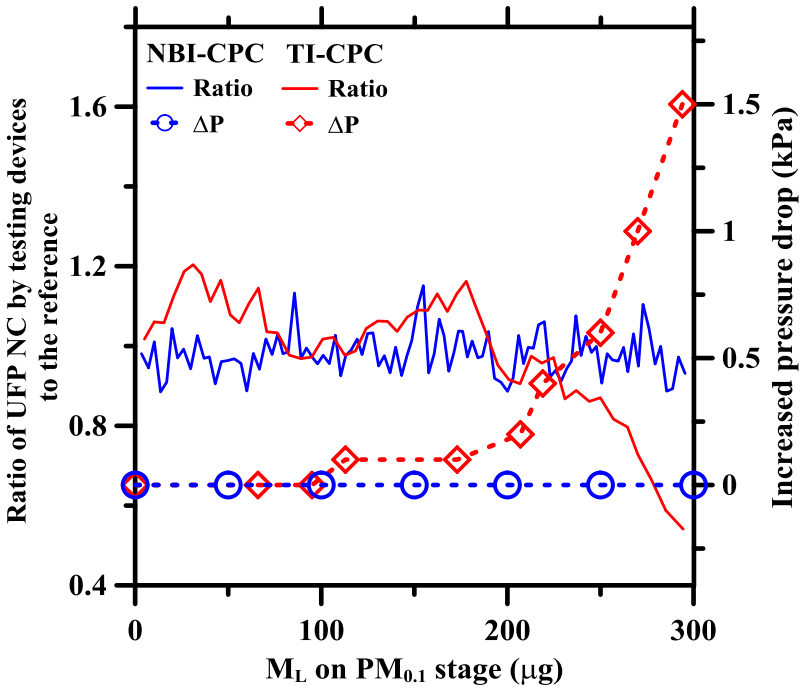

Fig. 6. The ratio of UFP NC by the NBI-CPC to that by the SMPS at various M_L

be 1.08±0.07 and 1.05±0.06 when the M_L is less than 100 μg and in the range of 100-200 μg, respectively. This indicates that the performance of the TI-CPC with a loaded mass of less than 200 μg is comparable to the SMPS. However, the ratio is decreased to 0.92 and 0.52 when the M_L is increased to 200 and 300 μg. The reduction in the ratio indicates the decrease in the $PM_{0.1}$ NC measured by the TI-CPC when the M_L increases. With the silicon oil-coated substrate, the particle mound is formed as evident by the increase in the pressure drop from 8.1 kPa to 8.3 and 15 kPa, respectively, at the M_L of 200 and 350 μg. As a result, more incoming particles are collected by the deposited particle mound, fewer particles enter the CPC and are measured.

In comparison, the $PM_{0.1}$ NBI-CPC with the water-wetted GFF substrate shows good performance for $PM_{0.1}$ NC measurement as the ratios of $PM_{0.1}$ NC to the SMPS are 0.97±0.05, 0.99±0.05, and 0.97±0.06 with the M_L in the range of 0-100, 100-200, and 200-300 μg,

449 respectively. The initial ratio is close to 1 and remains constant despite the increase in the M_L,
450 which implies that the NBI-CPC can measure $PM_{0.1}$ NC accurately without a particle loading
451 effect. This is due to the effective removal of particle deposits by water washing the
452 GFF-covered substrate. In addition, the constant pressure drop during the particle loading
453 process also supports the finding that there is no particle mound formed on the impaction
454 substrate.

455 In this study, the 3 L/min $PM_{0.1}$ NBI is also used to replace the TSI inlet impactor of the
456 SMPS as the $PM_{0.1}$ NBI-SMPS for the UFP size distribution measurement without particle
457 loading effect. The results show that the UFP size distribution measured by the $PM_{0.1}$
458 NBI-SMPS remains stable with the increase in the M_L up to 1.1 mg (see in the Fig. S8
459 (Section B) of the SI). The good cut-off characteristics of the NBI results in a size distribution
460 with a nearly ideal cut-off for particles smaller than 100 nm and the effective removal of
461 particle larger than 100 nm. These results demonstrate that 3.0 L/min $PM_{0.1}$ NBI can be a
462 viable classifying device for long-term monitoring for the SMPS with a minimum
463 maintenance need. In the future, the NBI with larger cut-sizes (such as $PM_{0.4}$ – $PM_{0.9}$ NBI
464 with 0.4-0.9 μm cut-sizes similar to those of the SMPS inlet impactors) can be designed to
465 replace the original SMPS inlet impactor to obtain unbiased aerosol size distributions, which
466 otherwise could be affected by particle bounce and loading effects.

467

468 *Field comparison test in the ambient condition*

469 Fig. 7 displays the correlation plot for $PM_{0.1}$ NCs measured by the 3 L/min $PM_{0.1}$
470 NBI-CPC and SMPS in the field test. To maintain the good performance of the SMPS which
471 was used as the reference, the SMPS impactor was cleaned daily. The results show that the
472 slope and R^2 of the linear regression lines of pairwise comparisons are 0.98 and 0.95,
473 respectively (No. of 5-min average data: 1440). The $PM_{0.1}$ NCs of the NBI-CPC ranges from
474 1,907 to 42,326 #/cm^3 during the 5-day monitoring period, which are close to those of the

SMPS (i.e. particles smaller than 100 nm) varying from 2,146 to 44,196 #/cm^3. This indicates a good agreement between the UFP NC measurement of the NBI-CPC and SMPS.

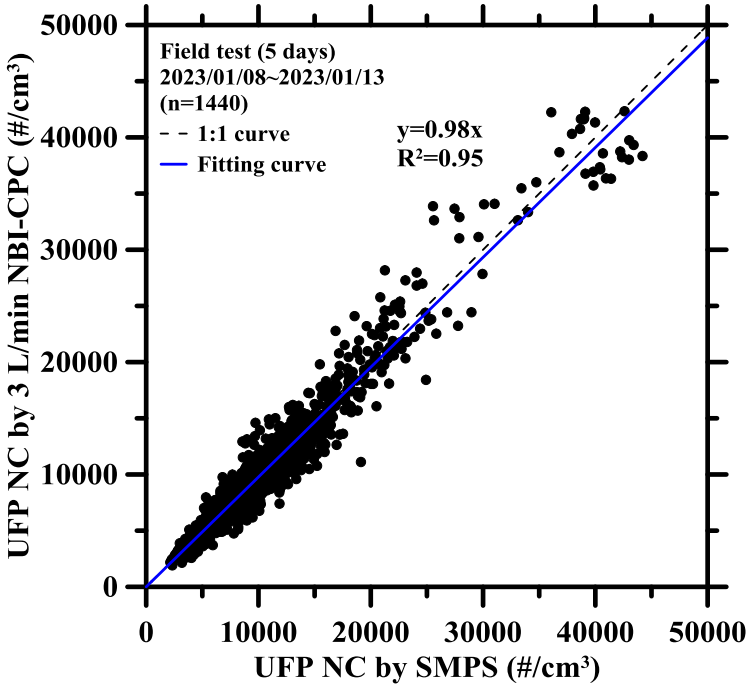

Fig. 7. Correlation plot for UFP NC by the NBI-CPC and SMPS with an inlet impactor cleaned daily in the field test

As shown in Fig. 8, both devices correlate very well at low concentrations and high peaks. The peak NC bias is less than 5% while the lowest NC bias is 11%. The measurement bias in low concentration ranges is attributed to the uncertainty of the CPC measurement limit and the SMPS scanning range limit. The uncertainty is 10% for particle concentrations of 1000 #/cm^3

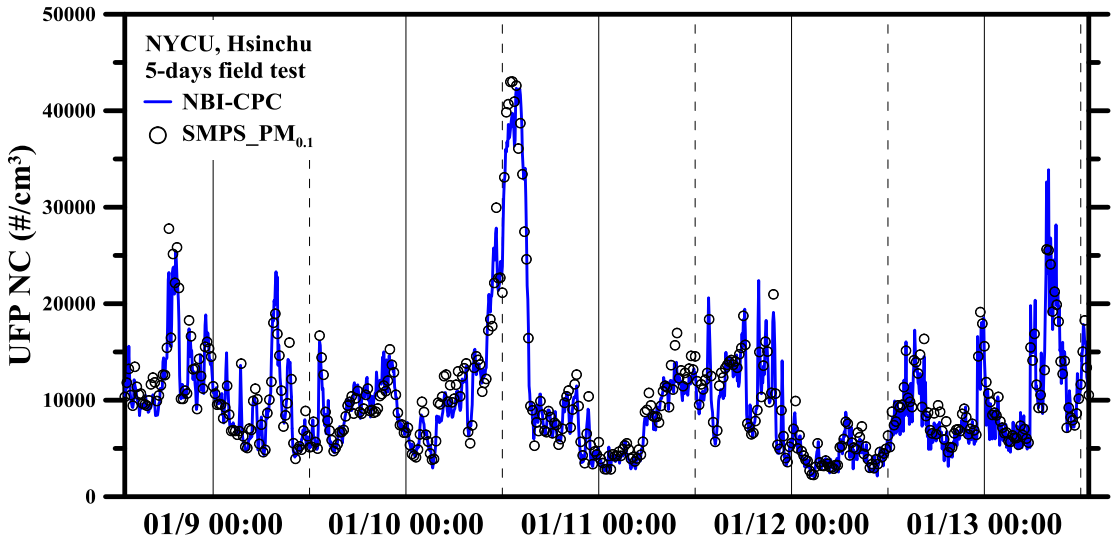

Fig. 8. Field comparison of the UFP NCs by NBI-CPC and SMPS

in the CPC according to the TSI manual, and 10% for particles with a D_{pe} ranging from 20 to 200 nm in the SMPS (Wiedensohler et al., 2012).

Note that even higher correlation of the two devices (slope = 0.99) can be achieved by changing the effective density from 1.2 to 1.3 g/cm^3 in the period of mid-noon (11:00 to 14:00) for converting SMPS D_{pe} -data to D_{pa}-data (Lin et al., 2018). It is reported that a higher effective density was found for particles with a high proportion of ammonium sulfate and ammonium nitrate salts formed during mid-noon owing to photochemical reactions (Yin et al., 2015). That is, the SMPS data can't be used to obtain the actual UFP NC directly due to some uncertainties in effective particle density. In contrast, the $PM_{0.1}$ NBI-CPC is a relatively convenient choice for obtaining UFP NC since the measurement is based on D_{pa}.

4. Conclusion

This study designed and tested a 30 L/min $PM_{0.1}$ non-bouncing impactor (30 L/min $PM_{0.1}$ NBI) and a NBIS ($PM_{0.1}$ non-bouncing impactor sampler, the $PM_{0.1}$ stage with 3 preceding stages) for accurate UFP MC measurement without the issues of particle loading and bounce. The NBI uses clean water to wet the GFF continuously, which prevents particle bounce and

helps remove deposited particles and provides a clean impaction surface without particle loading effect since particle loaded mass M_L on the substrate is essentially zero. In comparison, the impactor with a silicon oil-coated aluminum foil substrate has an obvious decreasing efficiency for particles larger than 300 nm due to particle bounce. The laboratory particle loading tests further show that the NBIS samples accurate UFP MCs with M_L on the $PM_{0.1}$ stage up to 21 mg with the difference of ca. 10%, while the traditional cascade impactor TCI-R over-measures MC initially due to initial particle bounce for particles larger than 300 nm and the over-estimation increases very much when the M_L exceeded 3 mg due to over-loading effect. In the ambient field tests, the UFP MCs of the NBIS differ by only ±0.5 $\mu g/m^3$ as compared to those of the rotating 10-stages NMCI (reference) while TCI-R also shows over-measurement by 0.8 $\mu g/m^3$ in average due to the bounce for particles larger than 300 nm. Furthermore, the TCI-NR shows higher over-measurement which increases further with increasing ambient concentration.

For the UFP NC measurement, the previously developed 3 L/min NIC (or called as 3 L/min $PM_{0.1}$ NBI in this study) is combined with a CPC as NBI-CPC, and it shows stable and accurate performance with M_L up to 300 μg, while the impactor with the non-rotating, silicone oil-coated substrate under-measures owing to over-collection for particles smaller than the cut-size when M_L exceeds 200 μg. In ambient field tests, the 3 L/min $PM_{0.1}$ NBI-CPC measures NCs in good agreement with the SMPS reference values, with a linear regression slope of 0.98 and an R^2 of 0.95, respectively. This study concludes that traditional impactors with silicon oil-coated substrate can over-measure and under-measure the UFP MCs and NCs, respectively, due to particle bounce and loading effects, and the use of the NBI devices developed in this study can eliminate these effects to provide accurate UFP measurements.

In the future, the 30 L/min $PM_{0.1}$ NBI can be used to obtain enough UFP mass of over 1000 μg for toxicity study in one day for high UFP MC environments of several tens or

thousands of μg/m^3, or several 30 L/min $PM_{0.1}$ NBIs can be arranged in parallel to provide a higher flow rate and longer sampling days when UFP MC is low at several μg/m^3 only. For long-term UFP NC measurement, the 3.0 L/min $PM_{0.1}$ NBI-CPC is a viable instrument with a minimum maintenance need. In the future, the NBI with smaller flow rate and larger cut-sizes (such as $PM_{0.4}$ – $PM_{0.9}$ NBI with 0.4-0.9 μm cut-sizes similar to those of the SMPS inlet impactors) can be designed to replace the original SMPS inlet impactor to obtain the unbiased aerosol size distributions without particle bounce and loading effects for long-term monitoring applications.

Acknowledgement

The support of the Taiwan National Science and Technology Council (contracts MOST 108-2221-E-009-076-MY3, MOST 110-2622-8-110-001, MOST 111-2622-8-110-004 and MOST 111-2221-E-A49-057-MY3), the Ministry of Education, and the Higher Education Sprout Project of National Yang Ming Chiao Tung University is gratefully acknowledged.

List of abbreviations

D_{pa}	Aerodynamic diameter	NC	Number concentration
D_{pa50}	Cutoff aerodynamic diameter	NIC	Nanoparticle inertial classifier
GFF	Glass fiber filter	NMCI	NCTU micro-orifice cascade impactor
MC	Mass concentration	PENS	Personal nanoparticle sampler
M_L	loaded particle mass	TCI	Traditional cascade impactor
MOUDI	Micro-orifice uniform deposit impactor	TCI-R	Traditional cascade impactor with rotating stages
NBI	Non-bouncing impactor	TCI-NR	Traditional cascade impactor

			with non-rotating stages
NBIS	Non-bouncing impactor sampler	UFP	Ultrafine particle

CRediT author statement

Wen-Cheng Gong: Data curation, Carrying out the experiment, Figure preparation, Writing, Reviewing, Editing and Finalizing the manuscript.

Nicolas Jidenko: Rewiewing and Conceptualization

Yang-Rei Li: Data curation, Carrying out the experiments, Figure preparation

Thi-Cuc Le: Data curation, Writing, Reviewing, Editing the manuscript

Jean-Pascal Borra: Conceptualization, Methodology and Rewiewing

Chuen-Jinn Tsai: Conceptualization, Reviewing and Editing the final manuscript

Reference

Abdillah, S. F., & Wang, Y. F. (2022). Ambient ultrafine particle ($PM_{0.1}$): sources, characteristics, measurements and exposure implications on human health. *Environ. Res.,* 115061.

Bateman, A.P., Belassein, H. & Martin, S.T. (2014). Impactor apparatus for the study of particle rebound: relative humidity and capillary forces. *Aerosol Sci. Technol.,* 48(1), 42-52.

Chang, C., Demokritou, P., Shafer, M., & Christiani, D. (2013). Physicochemical and toxicological characteristics of welding fume derived particles generated from real time welding processes. *Environ. Sci.: Process. Impacts,* 15(1), 214-224.

567 Chen, S. C., Tsai, C. J., Chou, C. C. K., Roam, G. D., Cheng, S. S., & Wang, Y. N. (2010a).
568 Ultrafine particles at three different sampling locations in Taiwan. *Atmos. Environ.,*
569 44(4), 533-540.
570 Chen, S. C., Tsai, C. J., Huang, C. Y., Chen, H. D., Chen, S. J., Lin, C. C., ... & Dzumbova, L.
571 (2010b). Chemical mass closure and chemical characteristics of ambient ultrafine
572 particles and other PM fractions. *Aerosol Sci. Technol.,* 44(9), 713-723.
573 Chen, M., Romay, F. J., & Marple, V. A. (2018). Design and evaluation of a low flow
574 personal cascade impactor. *Aerosol Sci. Technol.,* 52(2), 192-197.
575 Chien, C. L., Tien, C. Y., Liu, C. N., Ye, H., Huang, W. & Tsai, C. J. (2015). Design and
576 testing of the NCTU micro-orifice cascade impactor (the NMCI) for the measurement
577 of nanoparticle size distributions. *Aerosol Sci. Technol.,* 49(10), 1009-1018.
578 Feng, J. Q. (2016). A computational study of particle deposition patterns from a circular
579 laminar jet. arXiv preprint arXiv:1608.04605.
580 Furuuchi, M., Eryu, K., Nagura, M., Hata, M., Kato, T., Tajima, N., ... & Otani, Y. (2010).
581 Development and performance evaluation of air sampler with inertial filter for
582 nanoparticle sampling. *Aerosol Air Qual. Res.,* 10(2), 185-192.
583 Geiss, O., Bianchi, I., & Barrero-Moreno, J. (2016). Lung-deposited surface area
584 concentration measurements in selected occupational and non-occupational
585 environments. *J. Aerosol Sci.,* 96: 24-37.

He, M., & Dhaniyala, S. (2013). A multiple charging correction algorithm for scanning electrical mobility spectrometer data. *J. Aerosol Sci.,* 61: 13-26.

HEI Review Panel on Ultrafine Particles. (2013). Understanding the health effects of ambient ultrafine particles. HEI Perspectives 3. Boston, MA, HEI.

Huang, C. H., Tsai, C. J., & Shih, T. S. (2001). Particle collection efficiency of an inertial impactor with porous metal substrates. *J. Aerosol Sci.*, 32(9), 1035-1044.

Huang, C. H., Chang, C. S., Chang, S. H., Tsai, C. J., Shih, T. S., & Tang, D. T. (2005). Use of porous foam as the substrate of an impactor for respirable aerosol sampling. *J. Aerosol Sci.,* 36(11), 1373-1386.

Kumar, P., Kalaiarasan, G., Porter, A. E., Pinna, A., Kłosowski, M. M., Demokritou, P., ... & Dilliway, C. (2021). An overview of methods of fine and ultrafine particle collection for physicochemical characterisation and toxicity assessments. *Sci. Total Environ.,* 756, 143553.

Le, T. C. & Tsai, C. J. (2017). Novel non-bouncing $PM_{2.5}$ impactor modified from well impactor ninety-six. *Aerosol Sci. Technol.,* 51(11), 1287-1295.

Le, T. C., Fu, C. X., Sung, J. C., Li, Z. Y., Pui, D. Y., & Tsai, C. J. (2020). The performance of the $PM_{2.5}$ VSCC and oil-wetted M-WINS in long-term field sampling studies. *Atmos. Environ.,* 239, 117804.

Le, T. C. & Tsai, C. J. (2021). Inertial Impaction Technique for the Classification of

Particulate Matters and Nanoparticles: A Review. *KONA Powder Part. J.,* 38, 42-63.

Le, T. C., Lin, C. H., Gong, W.C., Ždímal, V., Pui, D.Y. & Tsai, C.J. (2022). Novel inertial impactor for nanoparticle classification without particle loading effect. *J. Aerosol Sci.,* 159, 105879.

Liao, B. X., Gong, W. C., Li, Z., & Tsai, C. J. (2019). A mass correction method for the aerosol particle mass analyzer to measure the particle mass of sub-50 nm nanoparticles. *Aerosol Sci. Technol.,* 53(9), 1056-1066.

Liu, C. N., Awasthi, A., Hung, Y. H., & Tsai, C. J. (2013). Collection efficiency and interstage loss of nanoparticles in micro-orifice-based cascade impactors. *Atmos. Environ.,* 69, 325-333.

Marple, V. A., Rubow, K. L. & Behm, S. M. (1991). A microorifice uniform deposit impactor (MOUDI): description, calibration, and use. *Aerosol Sci. Technol.,* 14, 434-446.

Misra, C., Kim, S., Shen, S., & Sioutas, C. (2002). A high flow rate, very low pressure drop impactor for inertial separation of ultrafine from accumulation mode particles. *J. Aerosol Sci.,* 33(5), 735-752.

Morawska, L., Ristovski, Z., Jayaratne, E. R., Keogh, D. U., & Ling, X. (2008). Ambient nano and ultrafine particles from motor vehicle emissions: Characteristics, ambient processing and implications on human exposure. *Atmos. Environ.,* 42(35), 8113-8138.

Ohlwein, S., Kappeler, R., Kutlar Joss, M., Künzli, N., & Hoffmann, B. (2019). Health

624 effects of ultrafine particles: a systematic literature review update of epidemiological
625 evidence. *Int. J. Public Health*, 64, 547-559.
626 Querol, X., Tobías, A., Pérez, N., Karanasiou, A., Amato, F., Stafoggia, M., ... & Alastuey, A.
627 (2019). Monitoring the impact of desert dust outbreaks for air quality for health
628 studies. *Environ. Int.*, 130, 104867.
629 Reischl, G. P., & John, W. (1978). The collection efficiency of impaction surfaces: a new
630 impaction surface. Staub - Reinhalt. Luft 1978, 38, 55.
631 Saleh, Y., Antherieu, S., Dusautoir, R., Y. Alleman, L., Sotty, J., De Sousa, C., ... &
632 Lo-Guidice, J. M. (2019). Exposure to atmospheric ultrafine particles induces severe
633 lung inflammatory response and tissue remodeling in mice. *Int. J. Environ. Res.*
634 *Public Health*, 16(7), 1210.
635 Sillanpää, M., Hillamo, R., Mäkelä, T., Pennanen, A. S., & Salonen, R. O. (2003). Field and
636 laboratory tests of a high volume cascade impactor. *J. Aerosol Sci.*, 34(4), 485-500.
637 Sotty, J., Garcon, G., Denayer, F. O., Alleman, L. Y., Saleh, Y., Perdrix, E., ... & Canivet, L.
638 (2019). Toxicological effects of ambient fine ($PM_{2.5-0.18}$) and ultrafine ($PM_{0.18}$)
639 particles in healthy and diseased 3D organo-typic mucocilary-phenotype models.
640 *Environ. Res.*, 176, 108538.
641 Tsai, C. J., & Cheng, Y. H. (1995). Solid particle collection characteristics on impaction
642 surfaces of different designs. *Aerosol Sci. Technol.*, 23(1), 96-106.

643 Tsai, C. J., Huang, C. Y., Chen, S. C., Ho, C. E., Huang, C. H., Chen, C. W., ... & Ellenbecker,
644 M. J. (2011). Exposure assessment of nano-sized and respirable particles at different
645 workplaces. *J Nanopart Res.*, 13, 4161-4172.
646 Tsai, C. J., Liu, C. N., Hung, S. M., Chen, S. C., Uang, S. N., Cheng, Y. S., & Zhou, Y. (2012).
647 Novel active personal nanoparticle sampler for the exposure assessment of
648 nanoparticles in workplaces. *Environ. Sci. Technol.,* 46(8), 4546-4552.
649 Tsai, C. J., Lin, G. Y., Liu, C. N., He, C. E., & Chen, C. W. (2012). Characteristic of
650 nanoparticles generated from different nano-powders by using different dispersion
651 methods. J Nanopart. Res., 14, 1-12.
652 Turner, J. R., & Hering, S. V. (1987). Greased and oiled substrates as bounce-free impaction
653 surfaces. J. Aerosol Sci., 18(2), 215-224.
654 USEPA (2019) Integrated science assessment (ISA) for particulate matter (final report,
655 December 2019). Washington (DC): Environmental Protection Agency
656 Wiedensohler, A., Birmili, W., Nowak, A., Sonntag, A., Weinhold, K., Merkel, M., ... &
657 Bastian, S. (2012). Mobility particle size spectrometers: harmonization of technical
658 standards and data structure to facilitate high quality long-term observations of
659 atmospheric particle number size distributions. *Atmos. Meas. Tech.,* 5(3), 657-685.
660 WHO (2021). Who global air quality guidelines: particulate matter ($PM_{2.5}$ and PM_{10}), ozone,
661 nitrogen dioxide, sulfur dioxide and carbon monoxide: executive summary, World

Health Organization.

Xue, W., Xue, J., Mousavi, A., Sioutas, C., & Kleeman, M. J. (2020). Positive matrix factorization of ultrafine particle mass ($PM_{0.1}$) at three sites in California. *Sci. Total Environ.,* 715: 136902.

Xue, W., & Kleeman, M. J. (2022). Comparison of size-resolved PM elements measured using aluminum foil and Teflon impaction substrates: Implications for ultrafine particle source apportionment and future sampling networks in California. *Sci. Total Environ.,* 156523.

Yin, Z., Ye, X., Jiang, S., Tao, Y., Shi, Y., Yang, X., & Chen, J. (2015). Size-resolved effective density of urban aerosols in Shanghai. *Atmos. Environ.,* 100, 133-140.